

Subcellular targeting and interactions among the *Potato virus X* TGB proteins

Timmy D. Samuels^{a,1}, Ho-Jong Ju^{a,1}, Chang-Ming Ye^{a,1}, Christy M. Motes^b,
Elison B. Blancaflor^b, Jeanmarie Verchot-Lubicz^{a,*}

^a Department of Entomology and Plant Pathology, Oklahoma State University, 127 Noble Research Center, Stillwater, OK 74078, USA

^b Plant Biology Division, Samuel Roberts Noble Foundation, Ardmore, OK 73401, USA

Received 19 March 2007; returned to author for revision 24 April 2007; accepted 3 May 2007

Available online 5 July 2007

Abstract

Potato virus X (PVX) encodes three proteins named TGBp1, TGBp2, and TGBp3 which are required for virus cell-to-cell movement. To determine whether PVX TGB proteins interact during virus cell–cell movement, GFP was fused to each TGB coding sequence within the viral genome. Confocal microscopy was used to study subcellular accumulation of each protein in virus-infected plants and protoplasts. GFP:TGBp2 and TGBp3:GFP were both seen in the ER, ER-associated granular vesicles, and perinuclear X-bodies suggesting that these proteins interact in the same subdomains of the endomembrane network. When plasmids expressing CFP:TGBp2 and TGBp3:GFP were co-delivered to tobacco leaf epidermal cells, the fluorescent signals overlapped in ER-associated granular vesicles indicating that these proteins colocalize in this subcellular compartment. GFP:TGBp1 was seen in the nucleus, cytoplasm, rod-like inclusion bodies, and in punctate sites embedded in the cell wall. The puncta were reminiscent of previous reports showing viral proteins in plasmodesmata. Experiments using CFP:TGBp1 and YFP:TGBp2 or TGBp3:GFP showed CFP:TGBp1 remained in the cytoplasm surrounding the endomembrane network. There was no evidence that the granular vesicles contained TGBp1. Yeast two hybrid experiments showed TGBp1 self associates but failed to detect interactions between TGBp1 and TGBp2 or TGBp3. These experiments indicate that the PVX TGB proteins have complex subcellular accumulation patterns and likely cooperate across subcellular compartments to promote virus infection.

© 2007 Elsevier Inc. All rights reserved.

Keywords: Potexvirus; Cell-to-cell movement; Plasmodesmata transport triple gene block

Introduction

Potex-, hordei-, beny-, peclu-, pomo-, and carlavirus genomes contain three overlapping open reading frames, termed the triple gene block (TGB), which encode proteins required for virus cell-to-cell movement (Gilmer et al., 1992; Memelink et al., 1990; Skryabin et al., 1988). The TGB proteins are named TGBp1, TGBp2, and TGBp3. It is often suggested that the TGB proteins interact with one another to transport viral RNA across plasmodesmata (Lauber et al., 1998; Lawrence and Jackson, 2001; Lough et al., 1998, 2000; Morozov and Solovyev, 2003; Morozov et al., 1999; Tamai and Meshi, 2001; Zamyatnin et al., 2004). There are four lines of evidence to support this model. First, swapping individual TGB proteins between beny- and

pecluviruses was unsuccessful, but exchanging the entire TGB between these viruses produced infectious hybrid viruses. These results suggest the TGB proteins interact with one another in a species specific manner (Angell et al., 1996; Lauber et al., 1998). Second, the results of microinjection studies indicated that the potexvirus TGBp1 protein chaperones viral RNA (vRNA) across plasmodesmata. In these studies, the TGBp2 and TGBp3 proteins acted as accessory factors promoting cell-to-cell movement of the TGBp1/vRNA complexes (Lough et al., 1998, 2000; Morozov and Solovyev, 2003). Third, the results of biolistic bombardment studies indicate that a potexvirus ribonucleoprotein complex containing TGBp1 and coat protein (CP) moves from cell-to-cell (Hsu et al., 2004; Lough et al., 2000), but TGBp2 and TGBp3 are not co-translocated with the complex across the plasmodesmata. Based on this observation, the TGBp2 and TGBp3 proteins were proposed to play a role in intracellular trafficking of the movement complex or interact with a docking site at the plasmodesmata

* Corresponding author. Fax: +1 405 744 6039.

E-mail address: verchot.lubicz@okstate.edu (J. Verchot-Lubicz).

¹ Contributed equally to this study.

(Lough et al., 2000). Finally, the beny- and hordeivirus TGB proteins co-localize in cell wall associated membrane-rich peripheral bodies (MRPBs) in plant cells studied using confocal and electron microscopy (Erhardt et al., 2000, 2005; Gorshkova et al., 2003; Lawrence and Jackson, 2001; Solovyev et al., 2000; Zamyatnin et al., 2002, 2004).

In several studies, GFP was fused to TGBp2 and TGBp3 and the fusion proteins were shown to associate with the endoplasmic reticulum (ER). TGBp2 has two transmembrane domains and a central conserved motif that lies in the ER lumen. GFP:TGBp2 was also shown, using confocal microscopy, to associate with granular vesicles which align actin filaments (Ju et al., 2005; Krishnamurthy et al., 2003; Mitra et al., 2003; Solovyev et al., 2000; Zamyatnin et al., 2002, 2004). Substitution of conserved residues within the central ER-luminal domain of TGBp2 eliminated GFP:TGBp2 association with granular vesicles but had no effect on its ER association (Ju et al., 2007). The same mutations inhibited virus cell-to-cell movement indicating that these granular vesicles play an important role in virus movement (Ju et al., 2007). Using electron microscopy it was shown that the granular vesicles are ER-derived structures which contain ribosomes and co-immunolabeled with GFP and BiP (an ER resident chaperone) antisera (Ju et al., 2005). Similar fluorescent granules were reported in cells expressing GFP fused to the TGB proteins of viruses belonging to other TGB containing genera but researchers have not yet confirmed whether these are vesicles similar to the PVX TGBp2-related structures (Erhardt et al., 2000; Gorshkova et al., 2003; Solovyev et al., 2000; Yelina et al., 2005; Zamyatnin et al., 2002, 2004). The combined observations led some researchers to suggest that TGB-containing viruses associate within the ER or granules to traffic the movement complex toward the periphery of the cell (Haupt et al., 2005; Ju et al., 2007; Lucas, 2006; Morozov and Solovyev, 2003; Zamyatnin et al., 2002).

The potexvirus TGB differs from viruses of other genera because the TGBp1 protein is a suppressor of RNA silencing (Baulcombe, 2002; Voinnet et al., 2000). PVX TGBp1 blocks systemic spread of the silencing signal (Voinnet et al., 2000). Mutations eliminating the PVX TGBp1 silencing suppression activity also inhibit virus cell-to-cell movement (Bayne et al., 2005), suggesting that silencing suppression is crucial for promoting virus plasmodesmata transport. In addition, there are several studies showing that PVX TGBp1 destabilizes virions and promotes viral RNA translation (Atabekov et al., 2000; Kiselyova et al., 2001, 2003; Rodionova et al., 2003). These results combined with the lack of direct proof that potexvirus TGB proteins form a complex led us to explore the possibility that the PVX TGBp1 protein might act independently of TGBp2 and TGBp3 proteins to promote virus cell-to-cell movement. Moreover, evidence that the pomovirus *Potato mop top virus* (PMTV) TGBp2 and TGBp3 proteins interact with each other but not with the TGBp1 suggests that TGB protein interactions might differ among the six TGB-containing virus genera (Cowan et al., 2002).

Prior investigations to determine how potexvirus proteins interact have relied on mutant PVX viruses, transgenic plants, or

plasmids expressing GFP fused TGB proteins from the CaMV 35S promoter (Krishnamurthy et al., 2002; Lough et al., 1998, 2000; Solovyev et al., 2000; Zamyatnin et al., 2002). In this study GFP was fused to each TGB protein and inserted into the PVX genome. We were able to track changes in the subcellular accumulation patterns of each TGB protein over space and time. To investigate whether the PVX TGB proteins interact with one another, as has been so often proposed, intrinsically fluorescent proteins (GFP, YFP, and CFP) were fused to each TGB gene and inserted either into pRTL2 or pSAT6 plasmids next to the CaMV35S promoter. Both *in vivo* expression systems showed the TGBp2 and TGBp3 fusions colocalize in several subdomains of the endomembrane network while TGBp1 fusions remained primarily in the nucleus and cytosol. In addition, direct protein–protein interactions were tested in yeast two hybrid experiments. The data presented in this study suggest that PVX TGBp1, similar to PMTV TGBp1, accumulates independently of TGBp2 and TGBp3 proteins (Cowan et al., 2002).

Results

PVX.GFP-TGBp2 and PVX.TGBp3-GFP have similar fluorescence patterns in plants

GFP was fused to PVX TGBp2 or TGBp3 coding sequences within the PVX genome (Fig. 1). GFP was used to visualize the subcellular distribution of each TGB protein during virus infection in tobacco leaves and protoplasts. PVX-GFP:TGBp2 has most of the endogenous TGBp2 coding sequence deleted and the fused genes were inserted into the viral genome next to a duplicated CP subgenomic promoter (Fig. 1). The GFP:TGBp2 fusions functionally replaced the deleted genes. In PVX-TGBp3:GFP, the GFP coding sequence was directly fused to the 3' end of the endogenous TGBp3 gene (Fig. 1).

N. benthamiana plants were inoculated with infectious transcripts, and infection foci on inoculated leaves were studied between 3 and 5 days post-inoculation (dpi), before virus spreads systemically. In PVX-GFP-infected cells, fluorescence was mainly cytosolic and nuclear. Fluorescent strands of cytoplasm were seen traversing the vacuole and around the periphery of the cell (Figs. 2A and B). Fluorescent amorphous bodies were also seen neighboring the nucleus. Some leaf segments were treated with DAPI to distinguish the nucleus from the surrounding amorphous body (Figs. 2C and D). These large perinuclear amorphous bodies are likely to be X-bodies described in previous studies from our laboratory and other laboratories. These X-bodies were described by electron microscopy to be rich in membranes and ribosomes and are likely to be centers for virus replication (Allison and Shalla, 1973; Espinoza et al., 1991; Ju et al., 2005; Kikumoto and Matsui, 1961; Kozar and Sheludko, 1969). In PVX-GFP-inoculated tobacco leaves there was no difference in the pattern of fluorescence seen in infected cells located at the center and leading edge of infection.

The patterns of fluorescence in PVX-GFP:TGBp2 (Figs. 3A–C) and PVX-TGBp3:GFP (Figs. 3D–F) infection foci were examined between 3 and 5 dpi and were similar. GFP:TGBp2

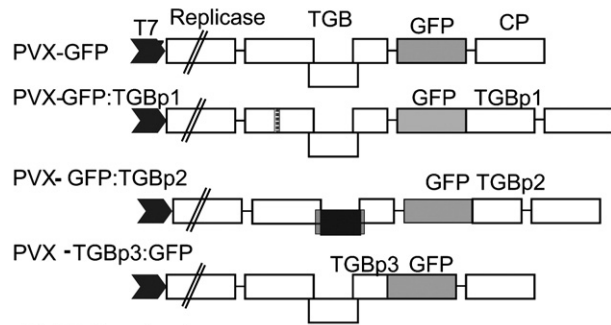
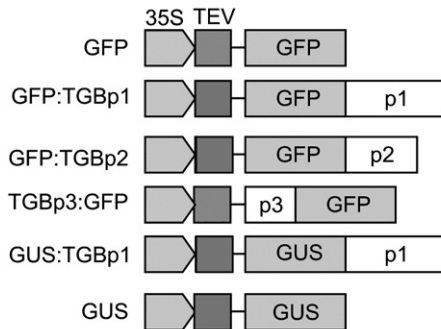
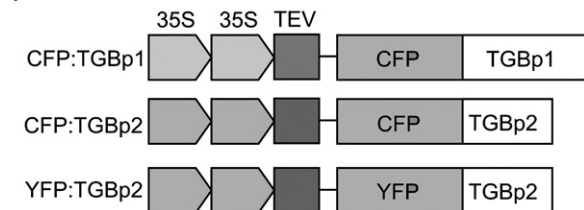
PVX infectious clones**pRTL2 Constructs****pSAT6 Constructs**

Fig. 1. Schematic of plasmids used in this study. The pPVX constructs contain PVX genomic cDNA inserted next to a bacteriophage T7 promoter (light gray arrow). Open boxes represent the PVX coding sequences. The replicase coding sequence is intersected by double lines, indicating that it is drawn shorter than to scale. The plasmid pPVX-GFP contains the EGFP coding sequence (gray box) next to a duplicated coat protein subgenomic promoter. The plasmids pPVX-GFP:TGBp1 and pPVX-GFP:TGBp2, contain the EGFP coding sequence fused to either the 5' end of the TGBp1 or TGBp2 coding sequences, respectively (Ju et al., 2005; Yang et al., 2000). The fused genes are next to the duplicated coat protein subgenomic promoter. In pPVX-GFP:TGBp1 has two stop codons introduced into the endogenous TGBp1 coding sequence (indicated by hatched box) which eliminates expression of the native TGBp1. The pPVX-GFP:TGBp2 lacks the coding sequence between nucleotide positions 5170 and 5423 (black box). Six pRTL2 constructs contain the CaMV 35S promoter (grey arrow), a TEV translation enhancer sequence (dark gray box), and either the GFP or GUS (gray box) coding sequences alone or fused to PVX TGBp1, TGBp2, or TGBp3 coding sequences. Three pSAT6 plasmids contain CFP or YFP (gray) fused to TGBp1 or TGBp2 coding sequences. The gray arrows represent tandem CaMV 35S promoters and the shaded boxes represent the TEV translation enhancer sequence.

and TGBp3:GFP fluorescence associated with the ER and fluorescent granules along the ER. In the case of TGBp2, these granules were shown to be ER-derived vesicles using electron microscopy (Ju et al., 2005). These results suggest that TGBp3 may colocalize with TGBp2 along the ER and in the granular vesicles.

In addition, GFP:TGBp2 and TGBp3:GFP were seen in large amorphous masses which were often near the nucleus (Figs. 3B

and E). These are likely to be X-bodies seen in PVX-GFP-infected cells in Fig. 2 (Ju et al., 2005). TGBp3:GFP fluorescence was also in the nucleus (Figs. 3G–I). We stained some PVX-TGBp3:GFP infection sites with DAPI to distinguish the nuclei from the perinuclear amorphous masses (Figs. 3G–I).

Essentially both GFP:TGBp2 and TGBp3:GFP fusions associated with several subdomains of the endomembrane system during PVX infection. While these data could be interpreted as evidence which supports earlier speculations that these proteins similarly function as membrane anchors for the viral movement complex (Lough et al., 2000; Morozov and Solovyev, 2003). Researchers suggested that these proteins tether a TGBp1/CP/vRNA complex to the ER, and the entire complex moves laterally along the ER toward the plasmodesmata, although a membrane bound movement complex has not yet been identified for PVX (Lough et al., 1998, 2000). On the other hand, evidence of both proteins in the ER, vesicles, and perinuclear masses raise the possibility that these proteins target to multiple subcellular domains and likely contribute to multiple steps in the infection cycle.

TGBp2 remains in vesicles while TGBp3:GFP accumulates in perinuclear masses in virus-infected protoplasts

Evidence that GFP:TGBp2 and TGBp3:GFP have the same subcellular targeting capacity in PVX-infected plants suggests that these proteins may interact in the endomembrane network to promote virus cell-to-cell movement. However, protein

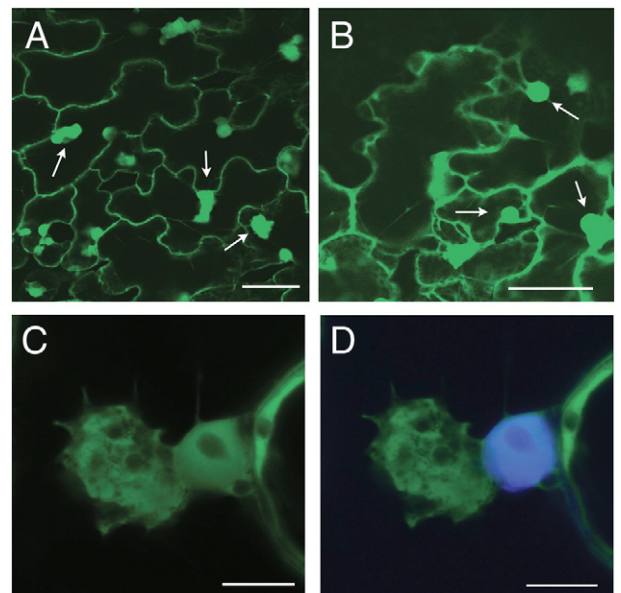


Fig. 2. Representative confocal images of plants inoculated with PVX-GFP-inoculated plants. (A, B) Images of PVX-GFP-infected cells at the center and leading edge of an infection site. GFP is characteristically expressed in the cytoplasm and nucleus. Large amorphous X-bodies are seen near the nucleus. Arrows point to the nucleus. (C, D) High resolution images shows amorphous X-body surrounding the nucleus. The infection site treated with DAPI shows blue fluorescence in the nucleus. Since the amorphous X-body surrounds the nucleus, DAPI staining helps to differentiate these separate structures. Scale bars in panels A, B represent 40 μ m. Scale bars in panels C, D represent 10 μ m.

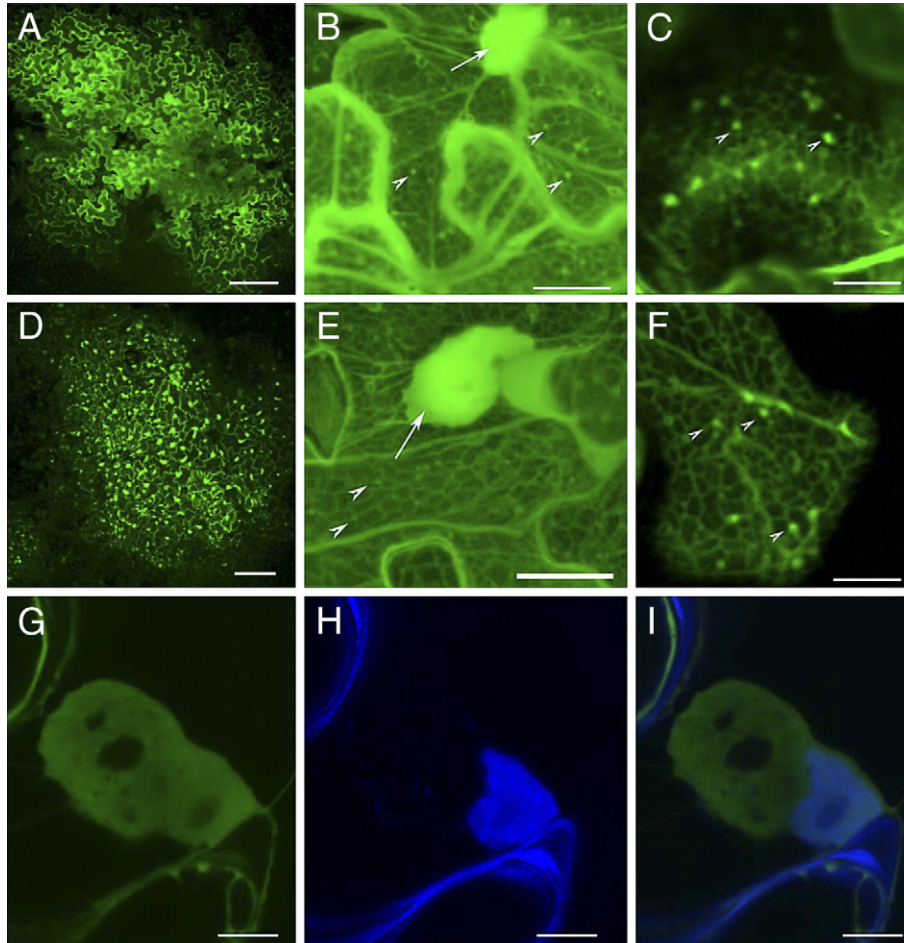


Fig. 3. Representative confocal images of PVX-GFP:TGBp2 and PVX-TGBp3:GFP-infected plants. (A, D) Low magnification images of PVX-GFP:TGBp2 and PVX-TGBp3:GFP infection sites on inoculated leaves seen at 5 dpi. (B, C) PVX-GFP:TGBp2-infected cells show fluorescence in the ER, ER-associated vesicles, and amorphous X-bodies. Arrows point to examples of X-bodies and arrowheads point to fluorescent granules which are likely ER-associated vesicles. (E, F) PVX-TGBp3:GFP-infected cells, similar to PVX-GFP:TGBp2, shows fluorescence in the ER, ER-associated fluorescent granules, and amorphous X-bodies. Arrowheads point to fluorescent granules. (G–I) High resolution images of amorphous X-body and nucleus in PVX-TGBp3:GFP-infected cell. Infected cells were treated with DAPI which shows blue fluorescence in the nucleus. Image shows that the amorphous bodies surround and overwhelm the nucleus as in PVX-GFP-infected cells. Scale bars in panels A, D represent 200 μm ; scale bars in panels B, E represent 40 μm ; and scale bars in panels C, F–I represent 10 μm .

sequences show some different properties which suggest these proteins function differently. TGBp2 has two transmembrane domains and a central conserved motif which resides in the ER lumen and regulates vesicle morphology (Mitra et al., 2003; Zamyatin et al., 2006). TGBp3 has an N-terminal transmembrane domain and a C-terminal cytosolic region which likely interacts with factors on the cytosolic face of the ER (Krishnamurthy et al., 2003). To determine if these proteins have different effects on the endomembrane system, we inoculated protoplasts with PVX-GFP:TGBp2 and PVX-TGBp3:GFP transcripts. While 3 dpi was the earliest time we could study spreading infection in plants, protoplasts provide the opportunity to study synchronously infected cells and conduct time course experiments to study changes in the patterns of GFP:TGBp2 and TGBp3:GFP accumulation earlier in virus infection. The fluorescence patterns seen in PVX-GFP:TGBp2 and PVX-TGBp3:GFP-infected protoplasts were different suggesting that early in virus infection these two proteins may initially target different subdomains of the

endomembrane network and later in infection appear throughout the same cellular compartments.

PVX-GFP:TGBp2 inoculated protoplasts were studied at 12, 24, 36, and 48 hpi. Between 12 and 48 hpi, GFP:TGBp2 fluorescence was mainly in the granular vesicles (Fig. 4) characterized in previous studies (Ju et al., 2005, 2007). The density of vesicles lining the plasma membrane and nuclear envelope appeared to increase over time (between 12 and 48 hpi). ER association and perinuclear amorphous masses were not detected in PVX-GFP:TGBp2 infected protoplasts suggesting that GFP:TGBp2 may accumulate to detectable levels in these locations much later in infection, as seen in plants at 3 dpi.

PVX-TGBp3:GFP inoculated protoplasts were studied at 12, 24, and 36 hpi (Fig. 5). TGBp3:GFP fluorescence associated with the nucleus and perinuclear amorphous masses. The most striking observation in PVX-TGBp3:GFP-infected protoplasts was that the amorphous masses appeared to grow over time. Specifically, at 12 hpi several small round

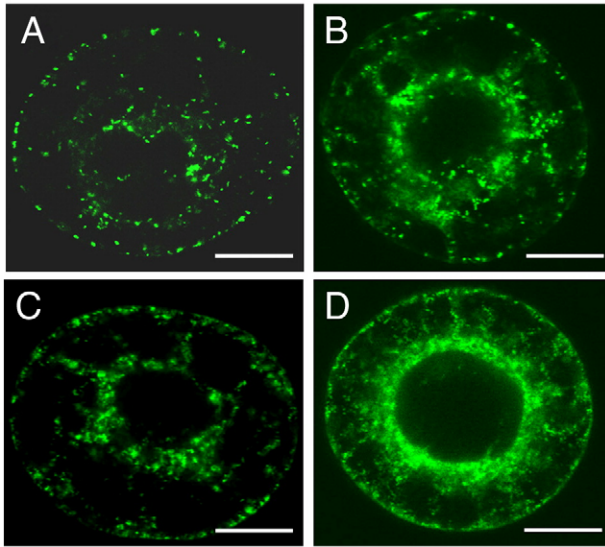


Fig. 4. Representative confocal images of PVX-GFP:TGBp2-infected protoplasts taken at (A) 12 hpi, (B) 24 hpi, (C) 36 hpi, and (D) 48 hpi. GFP:TGBp2 fluorescence occurs in the vesicles at each time point. Scale bar represents 10 μ m.

bodies were detected encircling the nucleus (Fig. 5A). These round bodies coalesced on one side of the nucleus at 24 hpi (Fig. 5B). Between 36 and 48 hpi, the amorphous mass grew and took up most of the volume of the cytoplasm (Figs. 5C and D). Some protoplasts were treated with ER-tracker dye at 36 and 48 hpi (Figs. 5E and F). ER-tracker dye and GFP fluorescence can be differentiated using an epifluorescence microscope. The pattern of ER-tracker fluorescence resembled the pattern of TGBp3:GFP fluorescence in the same cells, suggesting that these amorphous masses are rich in ER membranes (Figs. 5E and F). Thus TGBp3, but not TGBp2, appears to play a central role in the expansion of ER membranes forming the perinuclear amorphous masses.

These data suggest that TGBp2 and TGBp3 target different ER subdomains early in PVX infection. TGBp2 is first seen in granular vesicles while TGBp3 is first in the nucleus and amorphous masses. Since the TGBp2-related granular vesicles were previously shown to be ER derived (Ju et al., 2005, 2007), and the ER-tracker dye indicates the perinuclear masses are rich in ER, it is likely that over time both proteins appear in the same subcellular domains (seen in plants after 3 dpi) and may be due to their mutual association within the ER.

TGBp2 and TGBp3 fusion proteins colocalize in the ER and vesicles

To determine if TGBp2 and TGBp3 colocalize, tobacco leaves were bombarded with a combination of pRTL2 plasmids expressing CFP:TGBp2 and TGBp3:GFP (Fig. 6). Fluorescence was viewed between 18 and 24 h post-bombardment. Both fusion proteins were seen in the same granular bodies along the ER (Figs. 6A through F).

Prior studies also showed that GFP:TGBp2 containing vesicles are unrelated to the Golgi apparatus. DsRed-ST has

the signal anchor of a rat sialyl transferase fused to DsRed-2 and is targeted to the Golgi network (Dixit and Cyr, 2002). Cells expressing GFP:TGBp2 and DsRed-ST showed green and red fluorescence in separate vesicles. Moreover, immunogold labeling and electron microscopic analysis failed to detect GFP:TGBp2 or GFP:TGBp3 in Golgi vesicles (Ju et al., 2005). The GFP:TGBp2-related vesicles were studded with ribosomes, were unaffected by brefeldin A treatment (which dissolves the Golgi apparatus), and were immunolabeled with BiP antisera suggesting that they were ER-derived structures (Ju et al., 2005; Mitra et al., 2003). However, association of TGBp3:GFP with granular vesicles has not been previously explored. To further investigate whether TGBp3:GFP associates with the Golgi, plasmids expressing TGBp3:GFP and DsRed-ST were co-bombarded to tobacco leaves (Figs. 6G–I). DsRed-ST has the signal anchor of a rat sialyl transferase fused to DsRed-2 and is targeted to the Golgi network. A green network and red vesicles were seen in TGBp3:GFP and DsRed-ST expressing cells. The DsRed and GFP signals did not overlap, proving that TGBp3:GFP does not localize to the Golgi network (Fig. 6I).

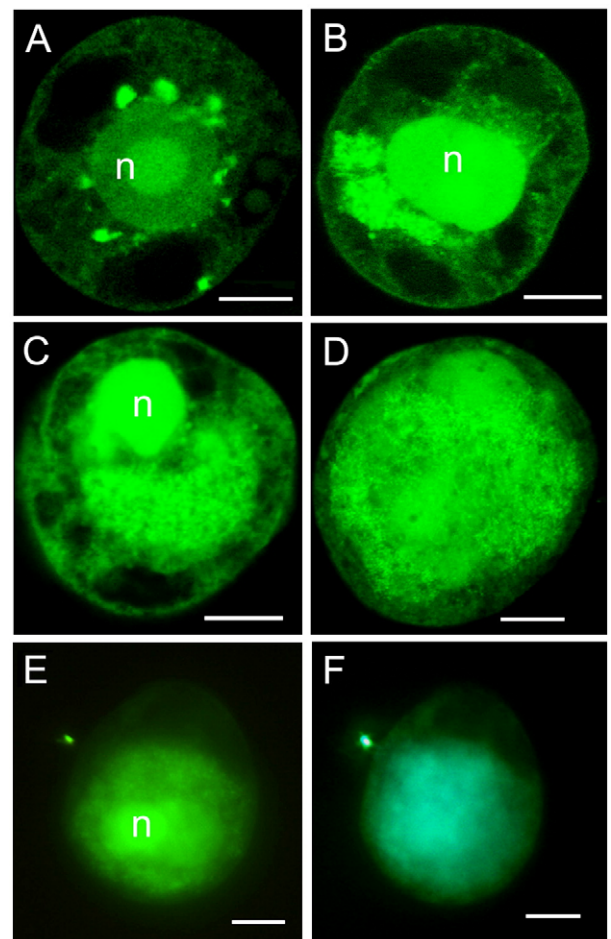


Fig. 5. Representative confocal images of PVX-TGBp3:GFP-infected protoplasts taken at (A) 12 hpi, (B) 24 hpi, (C) 36 hpi, and (D) 48 hpi. TGBp3:GFP fluorescence occurs in the nucleus at each time point. (E, F) Some PVX-TGBp3:GFP-infected protoplasts, harvested at 48 hpi, were treated with ER-tracker dye. (E) Green fluorescence and (F) ER-tracker dye fluorescence produced identical fluorescent patterns. Scale bar represents 10 μ m.

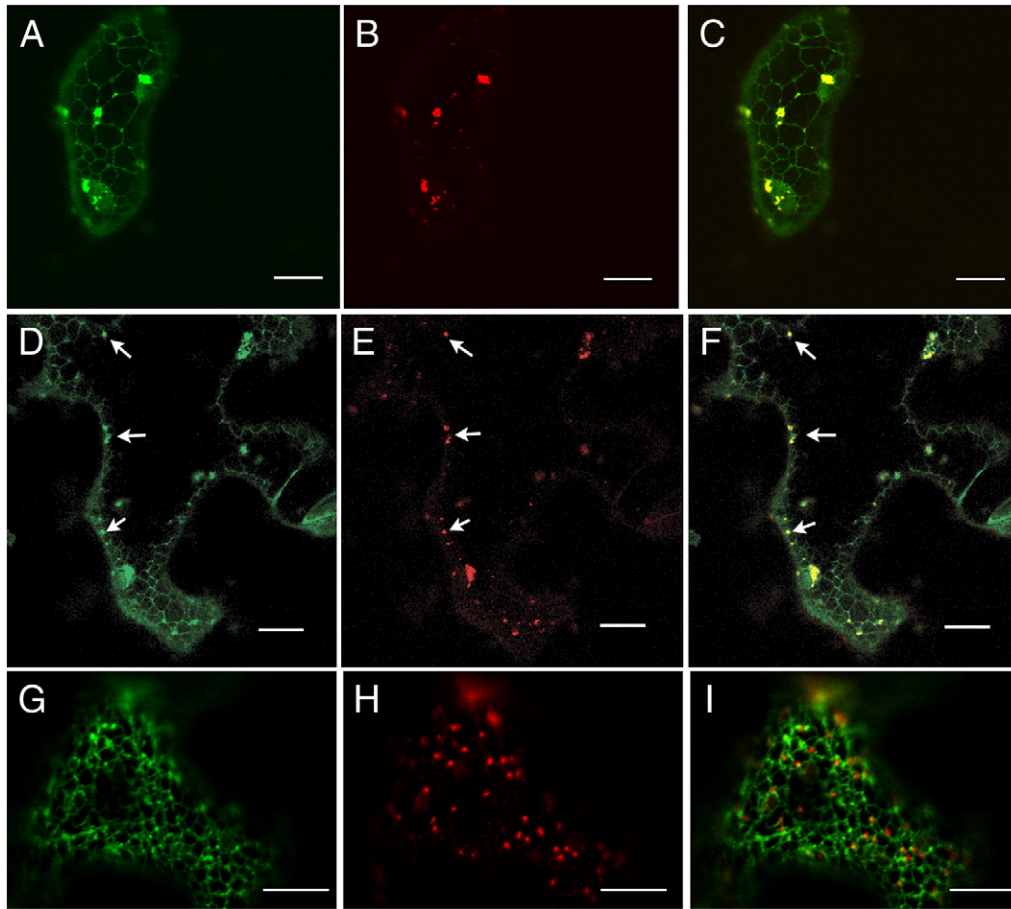


Fig. 6. Representative confocal images of CFP:TGBp2 and TGBp3:GFP expressing tobacco leaf epidermal cells. (A–C) Images show a single cell with red, green, and overlaid fluorescence. (D–F) A second example of a single cell with red, green, and overlaid fluorescence. TGBp3:GFP is in the ER. TGBp3:GFP and CFP:TGBp2 are in the same fluorescent granules. (G–I) Images of tobacco leaf epidermal cells bombarded with plasmids expressing TGBp3:GFP and DsRed-ST. DsRed-ST targets to the Golgi apparatus. Individual green and red fluorescence images, as well as the overlaid images (I), show green and red fluorescent signals do not colocalize. Thus, TGBp3:GFP does not move from the ER into the Golgi. Scale bars represent 20 μm .

Subcellular targeting of TGBp1 during virus infection in plants and protoplasts

Since TGBp2 and TGBp3 associate with the amorphous X-bodies, ER network, and granular vesicles during PVX infection, we conducted further investigations to find out if TGBp1 may also associate with the same structures. Based on previous models that TGBp2 and TGBp3 anchor the TGBp1 containing ribonucleoprotein complex (Lough et al., 1998, 2000; Morozov and Solovyeu, 2003), it is reasonable to consider that these proteins colocalize in one of the described subcellular domains. We fused GFP to the PVX TGBp1 and introduced the fusion into the PVX genome (Fig. 1). Most of the endogenous TGBp1 coding sequence was deleted from PVX-GFP:TGBp1 and the fused genes were inserted into the viral genome next to a duplicated CP subgenomic promoter (Fig. 1). The GFP:TGBp1 fusion functionally replaced the deleted gene.

PVX-GFP:TGBp1 infection in inoculated *N. benthamiana* leaves was delayed in comparison to PVX-GFP and we first observed infection sites at 5 dpi. The subcellular distribution of GFP:TGBp1 fluorescence in infection foci were compared between 5 and 8 dpi. The pattern of fluorescence in

PVX-GFP:TGBp1 infection sites was unlike GFP:TGBp2 and TGBp3:GFP fluorescence patterns. We studied sites that contained as few as two infected cells with larger sites containing 10 or more infected cells (Figs. 3A, B), which further aided comparisons of first infected cells with late infected cells. Faint cytosolic and nuclear fluorescence was evident in maximum projected images (Figs. 7A, B, and D). Rod-like projections were seen in many cells. The fluorescence signal in the rod-like structures was so intense that it was difficult to discern the structure of the body under normal imaging conditions and it was easy to assume they were the perinuclear amorphous masses seen in PVX-GFP, PVX-GFP:TGBp2, and PVX-TGBp3:GFP infected cells (compare Figs. 2 and 3B and E with Figs. 7B–D, and J). However, when we compared the amorphous masses seen PVX-GFP, PVX-GFP:TGBp2, or PVX-GFP:TGBp3 infected cells with the intensely fluorescent structures seen in PVX-GFP:TGBp1-infected cells at highest magnification and by reducing the voltage of the emissions detector there was a clear difference in their dimensions (compare Figs. 2C and 3G with Figs. 7A, E, and I). At highest resolution these structures often resembled elongated crystals (Fig. 7I), which were often overlapping each other and sometimes neighboring the nucleus

(Figs. 7A and D). Fluorescence was also in puncta embedded in cell walls throughout the infection site (Figs. 7A–D). These puncta are reminiscent of images seen in other confocal microscopy studies depicting viral movement proteins inside plasmodesmata. Similar cell wall puncta were described in studies of the PVX CP and TMV P30 movement protein to represent proteins which specifically localize to plasmodesmata (Crawford and Zambryski, 1999; Padgett et al., 1996;

Zambryski, 2004). Thus during PVX infection, GFP:TGBp1 is mainly in the nucleus, plasmodesmata, cytoplasm, and rod-like inclusions.

The pattern of PVX-GFP:TGBp1 fluorescence in inoculated protoplasts was similar to the virus-infected leaves. Fluorescence accumulated in the cytoplasm, rod-like projections, and nucleus at 12, 24, 36, 48 hpi (Figs. 7E, F). These rod-shaped inclusion bodies resemble previous reports of elongated inclusion bodies in PVX and *Foxtail mosaic virus* (FMV)-infected leaves (Davies et al., 1993; Rouleau et al., 1994).

We bombarded tobacco leaves and transfected protoplasts with pRTL2-GFP:TGBp1 plasmids and used epifluorescence microscopy to view GFP:TGBp1 fluorescence in the absence of virus infection. In bombarded leaves (data not shown) and protoplasts (Fig. 7J) GFP:TGBp1 was seen in the cytoplasm, nucleus, and in rod-like structures. Punctate spots were not seen in the cell walls of GFP:TGBp1 expressing cells, suggesting that this GFP:TGBp1 may require other viral factors to accumulate inside plasmodesmata. Since PVX CP produces the same punctate pattern, it is possible that TGBp1 requires the presence of CP during infection to localize in plasmodesmata.

The nuclear and cytosolic fluorescence in tobacco leaves inoculated with PVX-GFP:TGBp1 resembled the fluorescence pattern seen PVX-GFP-inoculated leaves. While it has been reported that GFP (27 kDa) is small enough to diffuse across the nuclear envelope, it seems less reasonable that GFP:TGBp1 (52 kDa) is also small enough to move passively across the nuclear envelope. Many studies have used GUS as a reporter to study nuclear trafficking. GUS is typically restricted to the cytoplasm, but can accumulate in the nucleus when fused to a nuclear targeting signal (Butterfield-Gerson et al., 2006; DeVries et al., 2002; Reiser et al., 1999; Restrepo et al., 1990). Therefore, protoplasts were transfected with pRTL2 plasmids expressing GUS or GUS:TGBp1 fused genes and then treated with the chromogenic substrate, 5-bromo-4-chloro-3-indolyl- β -D-glucuronic acid (X-gluc), which produces a blue precipitate. While the blue precipitate was mainly cytosolic in

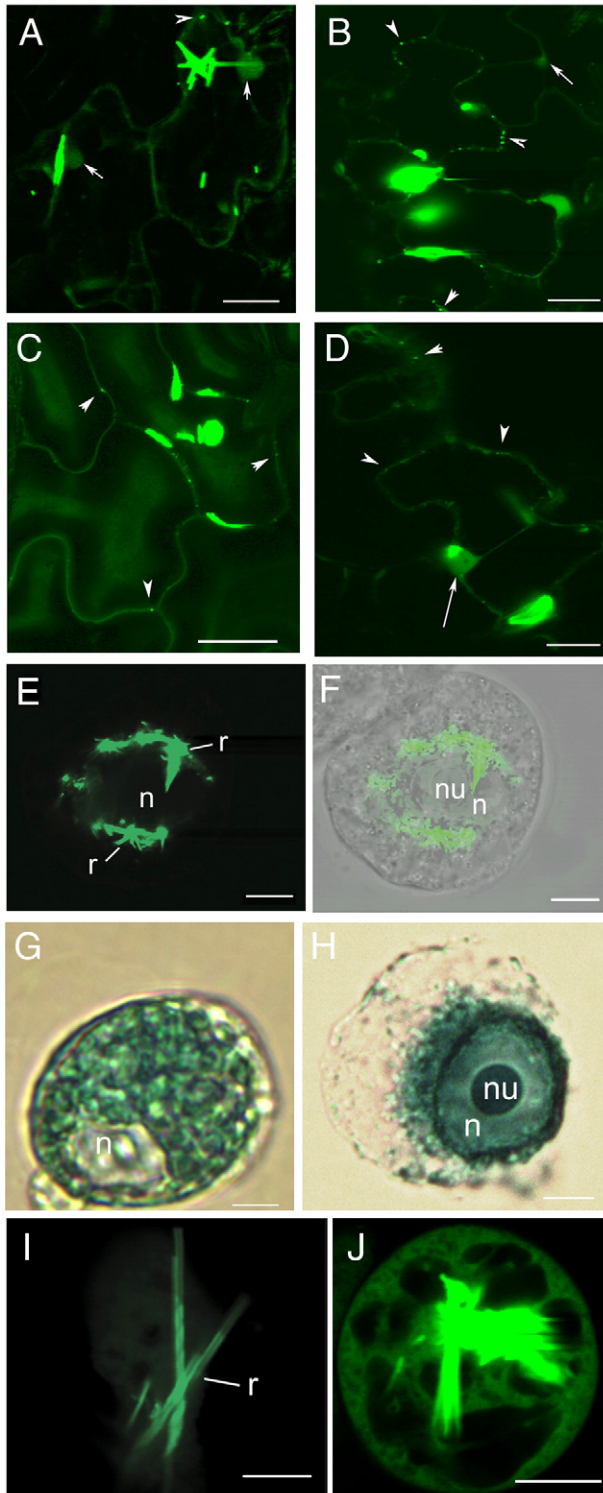


Fig. 7. Representative confocal images of plants and protoplasts inoculated with PVX-GFP:TGBp1. White arrows point to the nucleus in each panel. Arrowheads point to fluorescent spots embedded in the cell wall. (A) Infection site at 5 dpi shows faint levels of cytoplasmic fluorescence. Fluorescence is in overlapping rod-like structures which are sometimes near the nucleus. (B) Fluorescent infection site shows several adjacent cells. At the infection center fluorescence is associated with elongated structures, nucleus, and in spots in the cell wall. The cells at the top right are the furthest from the infection center and show fluorescence in the nucleus suggesting that early in infection GFP:TGBp1 is first seen in the nucleus. Rod-like structures accumulate later. (C, D) Additional images of neighboring PVX-GFP:TGBp1-infected cells. All infected cells show fluorescent spots in the cell wall, faint cytosolic fluorescence, and elongated rod-like structures. (E, F) PVX-GFP:TGBp1-infected protoplasts show rod-like structures surrounding the nucleus. (G, H) Images of GUS and GUS:TGBp1 expressing protoplasts, respectively. GUS is excluded from the nucleus (n) and nucleolus (nu) while GUS:TGBp1 shows blue precipitate inside the nucleus. (I) High resolution image of an elongated structure shows several overlapping cylindrical rods. (J) pRTL2-GFP:TGBp1 transfected protoplast shows cytoplasmic fluorescence and elongated rod-like structures overlapping the nucleus. Scale bars in panel A through panel D represent 40 μ m and the remaining panels contain scale bars that represent 10 μ m.

pRTL2-GUS transfected protoplasts, the blue precipitate was in the nucleus and cytoplasm of pRTL2-GUS:TGBp1 expressing protoplasts (Figs. 7G and H).

In summary, these data show that TGBp1 accumulates in four locations in PVX-infected cells. GFP:TGBp1 was seen in fluorescent puncta embedded in the cell walls, nucleus, cytoplasm, and rod-like structures.

Co-expression of PVX TGB proteins in bombarded tobacco leaves

CFP and YFP were also fused to each of the TGB proteins in plasmids adjacent to the CaMV 35S promoter (Fig. 1). Plasmids were co-bombarded to tobacco leaf epidermal cells and confocal microscopy was used to examine the subcellular distribution of the TGB proteins in relation to one another. Experiments using the recombinant PVX viruses suggest that TGBp1 accumulates separately from TGBp2 and TGBp3 during virus infection. By co-expressing TGBp1 with TGBp2 or TGBp3 in bombarded leaves, we could directly examine whether there were possibilities for TGBp1 to interact with TGBp2 or TGBp3. We also used the same plasmids to transfect protoplasts and the observations in protoplasts were similar to the observations made in bombarded leaves (data not shown). We tested all combinations of fusion proteins and the results were the same regardless of the combination of constructs used. A subset of the data is presented here.

In tobacco leaves and protoplasts expressing GFP:TGBp1 or CFP:TGBp1 fluorescence was mainly cytosolic and nuclear (Fig. 8A, data not shown). Many epidermal cells and protoplasts showed the elongated rod-like structures similar to those reported in PVX-GFP:TGBp1-infected cells (Fig. 7I). In tobacco leaves bombarded with plasmids expressing GFP:TGBp2, CFP:TGBp2 (data not shown), or YFP:TGBp2 (Fig. 8B), there was a consistent pattern of fluorescent vesicles scattered throughout the cell (Ju et al., 2005, 2007).

Plasmids expressing CFP:TGBp1 and YFP:TGBp2 were co-bombarded to tobacco leaf epidermal cells. Yellow fluorescent granular vesicles were seen along blue strands of cytoplasm stretching across the vacuole from the perinuclear region to the periphery of the cell (Figs. 8C and D). It is reasonable to consider that the cytosolic CFP:TGBp1 may aid in the long distance transfer of YFP:TGBp2-related vesicles from the perinuclear region to the outer edges of the cell. Importantly, CFP:TGBp1-related fluorescence was never detected inside the vesicles when examined at highest magnification. Thus, there is no evidence indicating TGBp1 accumulates inside the vesicles or forms a vesicle-bound complex with TGBp2. In addition YFP:TGBp2 was not found to associate with the elongated TGBp1-related rod-like projections (data not shown).

In epidermal cells bombarded with TGBp3:GFP containing plasmids, fluorescence was in the ER network (Figs. 8E and F) and formed a halo around the nucleus which is likely to be the perinuclear ER (Fig. 8G). Leaves were co-bombarded with CFP:TGBp1 and TGBp3:GFP and the images shown in Fig. 8 show red pseudocolor representing CFP:TGBp1 and green color representing TGBp3:GFP. Yellow signal appears where

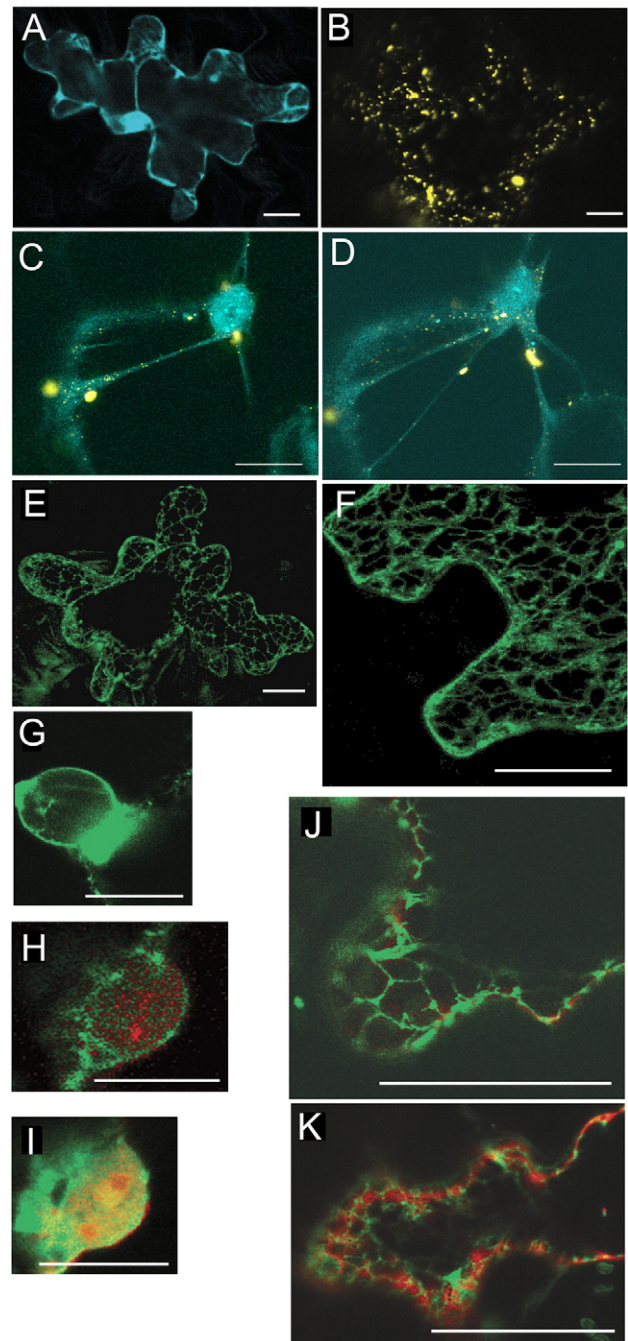


Fig. 8. Representative confocal images of tobacco leaf epidermal cells viewed 18–24 h post-bombardment with plasmids. Most images are maximal projections of a series of single plane images. (A) Example of a CFP:TGBp1 expressing cell showing nuclear and cytosolic fluorescence. (B) Example of YFP:TGBp2 expressing cell shows yellow granular vesicles (C, D) CFP:TGBp1 and YFP:TGBp2 expressing cell show blue fluorescence in the cytoplasm and yellow fluorescent vesicles. (E and F) TGBp3:GFP expressing cells show fluorescence in the cortical and perinuclear ER. (G) High magnification image shows TGBp3:GFP fluorescence in perinuclear ER. (H and I) TGBp3:GFP and CFP:TGBp1 expressing cells show both proteins target the nucleus. TGBp3:GFP is in the nuclear envelope while CFP:TGBp1 is inside the nucleus. (J and K) In cortical regions of the cell, TGBp3:GFP and CFP:TGBp1 show red cytoplasmic fluorescence due to CFP:TGBp1 surrounding the green fluorescent ER network containing GFP:TGBp3. Scale bars in panel A through F represent 20 μ m, and scale bars in panel G through K represent 10 μ m.

these two proteins colocalize. CFP:TGBp1 appeared to be inside the nucleus and TGBp3:GFP in the surrounding envelope (Figs. 8H and I). The signals sometimes overlapped in the nucleus. CFP:TGBp1 was also apparent in the cytoplasm and the TGBp3:GFP produced fluorescence in the ER network. At the edge of the cell, fluorescence due to CFP:TGBp1 surrounded the ER network, as expected of a cytoplasmic protein (Figs. 8J and K). While these two fusion proteins seemed to be in the same neighborhood, there was no clear evidence to indicate that CFP:TGBp1 was embedded in the ER when co-expressed with TGBp3:GFP. Similarly, TGBp3:GFP fluorescence was not found in the cytoplasm. Thus, looking at the relationship of cytoplasmic CFP:TGBp1 with YFP:TGBp2 or TGBp3:GFP, there are opportunities for these proteins to mingle or transiently interact, but there is no direct evidence that TGBp1 is part of a vesicle bound or ER bound complex. This is contrasted by experiments where CFP:TGBp2 and TGBp3:GFP were co-bombarded to tobacco leaves.

TGBp1 does not interact with TGBp2 or TGBp3 in yeast two hybrid assays

The BD Matchmaker GAL4 Two Hybrid System (Clontech) was also used to determine if TGBp1 interacts with TGBp2 or TGBp3 proteins. TGBp1, TGBp2, and TGBp3 were fused to the transcriptional activating domain (AD) and DNA-binding domain (BD) of GAL4, a yeast transcription factor (Fig. 9). Interactions between these proteins activate three reporter genes: *HIS3*, *ADE2*, and *MEL1*. Activation of the *HIS3* and *ADE2* reporter genes allows the host yeast to grow on nutritional medium lacking His or Ade. Activation of *MEL1* (*lacZ*) produces a blue precipitate when X- α -Gal was added to the medium (Fig. 9). The AD plasmids carry the Leu nutrient marker and the BD plasmids carry the Trp nutrient marker. Therefore, yeast transformed with AD and BD fusion constructs can be identified by growing on Leu⁻, Trp⁻ selection medium.

Initial transformants which grew on Leu⁻, Trp⁻ medium were re-streaked onto the more stringent Leu⁻, Trp⁻, His⁻, and Ade⁻ medium (Table 1; Fig. 9). The same colonies which grew










AD	BD	α -galactosidase assay
Tantigen	p53	blue 
CP	CP	blue 
TGBp1	TGBp1	blue 
TGBp1	TGBp3	white 
TGBp3	TGBp3	white 
-	TGBp1	white 
-	TGBp2	white 
-	TGBp3	white 
-	CP	white 

Fig. 9. Yeast two hybrid experiments to detect interactions among PVX TGB proteins. When AD and BD fusion proteins interact they reconstitute a transcription factor that binds to the GAL4 UAS domain and activates expression of *lacZ*. AD and BD fusions are listed. X- α -gal was added to the medium producing a blue precipitate when the AD and BD fusions interact. The colonies remain white when the fusion proteins do not interact. Boxes on the right show the blue and white colonies.

Table 1

Reporter assays using yeast co-transfected with plasmids expressing PVX proteins fused to the GAL4 activation domain (AD) or DNA binding domain (BD)

PVX genes fused to the GAL4 domains ^a		His and Ade ^b independent growth	Histochemical assay ^c (X- α -GAL)
AD	BD		
pCL	-	NA	+++
Tantigen	p53	+++	+++
TGBp1	-	NA	-
TGBp3	-	NA	-
CP	-	NA	-
-	TGBp1	-	-
-	TGBp2	-	-
-	TGBp3	-	-
-	CP	-	-
CP	CP	+++	+++
TGBp1	TGBp1	+++	+++
TGBp1	TGBp2	-	-
TGBp1	TGBp3	-	-
TGBp3	TGBp1	-	-
TGBp3	TGBp3	-	-

^a Clontech Matchmaker GAL4 two-hybrid system 3 uses two plasmids containing PVX genes fused either to the GAL4 activation domain (AD) or the DNA-binding domain (BD). Interactions between the target and bait proteins induce expression of *HIS3*, *ADE2*, and *lacZ*.

^b Yeast containing AD plasmids grows on medium lacking Leu. Yeast containing BD plasmids grows on medium lacking Trp. Yeast containing AD and BD plasmids grow on Leu⁻, Trp⁻ medium. Yeast were transfected with two plasmids and plated on Leu⁻, Trp⁻ medium. Then selected colonies were streaked onto Leu⁻, Trp⁻, His⁻, and Ade⁻ medium. NA = transfected yeast not tested for His and Ade independent growth. “+++” indicates yeast colonies which grew on His⁻, Ade⁻ medium. “-” indicates yeast colonies which did not grow on His⁻, Ade⁻ medium.

^c X- α -gal was added to Leu⁻, Trp⁻ medium or to Leu⁻, Trp⁻, His⁻, and Ade⁻ medium. Yeast colonies were re-streaked onto both types of medium. “+++” indicates yeast colonies which were blue. “-” indicates yeast which did not have a blue histochemical stain.

on Leu⁻, Trp⁻ medium were also streaked onto medium containing X- α -Gal (Table 1; Fig. 9). As expected, yeast transformed with only AD or BD plasmids did not grow on stringent Leu⁻, Trp⁻, His⁻, and Ade⁻ medium (Table 1).

Two positive controls were included in this study. First was the SV40 T-antigen and murine p53, which are known interacting factors provided by the BD Matchmaker kit. A second control was PVX CP fused to each AD and BD plasmids. The PVX CP was selected as a positive control because we know it forms oligomers on the way to forming virions.

Yeast colonies expressing T-antigen-AD and p53-BD, CP-AD and CP-BD, or TGBp1-AD and TGBp1-BD grew on stringent Leu⁻, Trp⁻, His⁻, and Ade⁻ medium and produced positive results in α -galactosidase assays. T antigen-p53, PVX CP-CP, and PVX TGBp1-TGBp1 interactions were detected using the yeast two hybrid assay (Table 1; Fig. 9). Yeast expressing TGBp1-AD and TGBp2-BD, TGBp1-AD and TGBp3-BD, TGBp3-AD and TGBp1-BD, or TGBp3-AD and TGBp3-BD grew on Leu⁻, Trp⁻ medium but did not grow on Leu⁻, Trp⁻, His⁻, and Ade⁻ medium (Table 1; Fig. 9). The α -galactosidase assays detected TGBp1-TGBp1 interactions

but were negative for TGBp1–TGBp2 or TGBp2–TGBp3 interactions (Table 1; Fig. 9). Thus, using the yeast two hybrid assay, we were unable to detect interactions between TGBp1 and TGBp2 or TGBp3. There was no evidence of TGBp3–TGBp3 interactions. Differences seen in the subcellular accumulation patterns of GFP:TGBp2 or TGBp3:GFP in transient assays and during virus infection may not be due to a stable interaction with or a dominant effect of TGBp1 but may depend on other viral or cellular factors.

Discussion

This is the first study to compare the subcellular accumulation patterns all three PVX TGB proteins during virus infection by fusing GFP to each of the respective coding sequences within the viral genome. Prior studies have co-delivered PVX viruses with plasmids expressing the GFP fusions into leaves (Morozov et al., 1999; Schepetilnikov et al., 2005). By expressing the fusions from the viral genome provides the opportunity to identify interactions among the viral proteins which may occur only in *cis*. There have been many studies, some of which were described in the introduction, attempting to characterize interactions among the TGB proteins. While TGBp1 has been shown to bind nucleic acids (Kalinina et al., 1996, 2002; Morozov et al., 1999; Rouleau et al., 1994) and interact with virions (Kiselyova et al., 2003), there is no published study showing that TGBp1 directly binds TGBp2 or TGBp3. In this study, we expected that the subcellular targeting patterns of each GFP fusion, when studied in the context of PVX infection, would produce similar subcellular targeting patterns if the TGB proteins form a complex. The results presented here demonstrated that PVX TGBp2 and TGBp3, but not TGBp1, colocalize in several subdomains of the endomembrane system.

In cells co-expressing CFP:TGBp1 with YFP:TGBp2 or TGBp3:GFP, the TGBp1 fusion remained in the cytoplasm and we found no evidence of TGBp1 being incorporated into vesicles or becoming embedded in the ER. Thus, if TGBp1 is interacting with TGBp2 or TGBp3 during virus infection the interactions may be transient or occur in a manner that does not alter the presence of TGBp1 in the cytoplasm. Yeast two hybrid experiments showed TGBp1–TGBp1 interactions but showed no evidence of TGBp1 forming a stable complex with TGBp2 or TGBp3. A related study of PMTV failed to detect interactions between TGBp1 and the other TGB proteins (Cowan et al., 2002). Yeast two hybrid experiments conducted using the PMTV TGB proteins similarly showed TGBp1 self-interacts but failed to detect interactions between TGBp1 and TGBp2 or TGBp3. The PMTV TGBp2 protein was shown to bind RNA and it was proposed that the membrane bound TGBp2 and TGBp3 proteins cooperated to transport viral RNA to the plasmodesmata (Cowan et al., 2002). The report suggests that the TGB protein complex is stabilized by TGBp1 and TGBp2 both binding the same RNA molecules (Cowan et al., 2002). Based on the results presented here, it is reasonable to consider that the model proposed for PMTV may also apply to PVX.

Protoplast experiments provided the first description of TGBp3:GFP accumulate during early stages of PVX infection which is strongly contrasted by the data obtained for PVX-GFP: TGBp2 presented here and in previous studies (Ju et al., 2005, 2007). Prior work suggested these vesicles might be TGBp2 induced structures derived from the perinuclear and cortical ER (Ju et al., 2005). On the other hand, TGBp3:GFP seems to associate mainly with the ER early in PVX infection and may even play a role (along with other factors) in stimulating membrane proliferation around the nucleus resulting in the X-bodies seen later in virus-infected leaves. TGBp3 cannot be solely responsible for causing the membrane proliferations since we do not observe similar masses growing in pRTL2-TGBp3:GFP transfected cells. But if these masses were centers for virus replication it is then reasonable to think that TGBp3 along with the viral replicase or other factors may work in concert to stimulate membrane proliferation. Thus, both TGBp2 and TGBp3 target the ER but have different effects on the ER. Later in infection, as seen in plants, both proteins seem to colocalize and so it appears that both proteins spread throughout the perinuclear and cortical ER and become incorporated into the same structures.

The subcellular targeting pattern of GFP:TGBp2 and TGBp3:GFP were almost identical in virus-infected leaves. The PVX TGBp2 and TGBp3 proteins were seen along the nuclear envelope, tubular ER traversing the vacuole and below the plasma membrane, granular vesicles along the ER, and amorphous masses surrounding the nucleus (Ju et al., 2005, 2007; Mitra et al., 2003; Schepetilnikov et al., 2005). The granular bodies associated with the ER in PVX-GFP:TGBp2-infected cells were described in prior electron and confocal microscopy studies to be ER-derived vesicles (Ju et al., 2005, 2007). These vesicles contain ribosomes, were unaffected by brefeldin A treatment (which dissolves Golgi), and were immunolabeled with BiP antisera (Ju et al., 2007; Mitra et al., 2003). In cells bombarded with CFP:TGBp2 and TGBp3:GFP the fluorescent signals colocalized in the granular vesicles. Since neither TGBp2 nor TGBp3 was seen to associate with the Golgi, these vesicles are likely to be the same ER-derived vesicles reported in studies of TGBp2 to be essential for virus cell-to-cell movement.

The amorphous masses seen in PVX-GFP, PVX-GFP:TGBp2, and PVX-TGBp3:GFP-infected cells were often surrounding the nucleus. PVX-TGBp3:GFP-infected protoplasts were stained with ER-tracker dye and the masses appeared to be rich in ER membranes (Fig. 5F). The masses grew from minor proliferations surrounding the nucleus to larger bodies which overwhelmed the entire protoplast. Similar masses were not seen in PVX-GFP or PVX-GFP:TGBp2 infected protoplasts suggesting that TGBp3 either plays a role in stimulating their formation or preferentially targets to these masses early in infection. Prior electron microscopic studies also described X-bodies growing from small perinuclear spherical bodies, rich in rough ER, to larger masses which can occupy large portions of the cell (Allison and Shalla, 1973; Kikumoto and Matsui, 1961; Kozar and Sheludko, 1969). Electron microscopic studies reported X-bodies occurring near

the nucleus and are oval or amorphous. Sometimes they appear as spongy masses with vacuolated areas as seen in Fig. 3G (Allison and Shalla, 1973; Kikumoto and Matsui, 1961; Kozar and Sheludko, 1969).

Studies of TMV and CaMV reported X-bodies to be centers for virus replication and translation (Buck, 1999; Espinoza et al., 1991). Since we see GFP as well as GFP:TGBp2 and TGBp3:GFP inside these structures, it is reasonable to consider that X-bodies may similarly function as a center for PVX protein synthesis. Further research is needed to determine if the X-bodies serve as a center for PVX replication, similar to the X-bodies described for TMV and CaMV (Buck, 1999; Espinoza et al., 1991).

The fluorescent puncta embedded in the cell wall of PVX-GFP:TGBp1 infected cells (Fig. 7) resembled the cell wall puncta first reported in TMV-infected tobacco leaves (Crawford and Zambryski, 2001; Oparka et al., 1997, 1999) and later shown in PVX-infected cells expressing GFP:CP fusions. Electron microscopy studies showed this fluorescence pattern is indicative of TMV MP or PVX GFP:CP targeted to plasmodesmata (Oparka et al., 1996, 1997, 1999; SantaCruz et al., 1996, 1998). Recent electron microscopic studies showed immunogold labeling identified the TGBp1 of *Peanut clump virus* (PCV) and *Beet necrotic yellow vein virus* (BNYVV) accumulating inside plasmodesmata (Erhardt et al., 1999, 2005). Similar to PVX, the BNYVV TGBp1 did not localize to plasmodesmata when expressed from plasmids in the absence of virus infection (Erhardt et al., 2005). For PVX, the CP is the likely candidate contributing to plasmodesmata targeting of TGBp1. The PVX CP was shown to accumulate inside plasmodesmata but does not induce gating. Perhaps PVX TGBp1 and CP form a docking complex within plasmodesmata regulating PVX cell-to-cell transport (Angell et al., 1996; Howard et al., 2004; Lough et al., 2000; Oparka et al., 1996). In this case, TGBp1 targeting to plasmodesmata is independent of TGBp2 and TGBp3.

TGBp1 was first shown to associate with elongated rod-like inclusions in electron microscopy studies using PVX-infected tissues (Davies et al., 1993; Hsu et al., 2004; Rouleau et al., 1994). Thus, the elongated structures seen here under the confocal microscope are typical of the PVX TGBp1 inclusions described in earlier literature. These rod-like structures have no known function and likely form by the aggregation of proteins expressed in excess.

The PVX TGBp1 is a suppressor of RNA silencing and like many other suppressors appears to accumulate inside the nucleus. A blue precipitate due to GUS:TGBp1 was also found in the nucleus and cytoplasm of transfected protoplasts. PVX TGBp1 resembles the *Cucumber mosaic virus* (CMV) 2b, *Tomato bushy stunt virus* (TBSV) 19K, *Begomovirus* AL2, and *Cucurtovirus* L2 proteins, which are silencing suppressors that are present in both the nucleus and cytoplasm of virus-infected cells (Canto et al., 2006; Lucy et al., 2000; Uhrig et al., 2004; Wang et al., 2003). The TBSV P19 protein interacts with nuclear ALY proteins which, in animals, regulate nuclear export of RNAs (Canto et al., 2006; Uhrig et al., 2004). The AL2 protein targets adenosine kinase (Wang et al., 2003, 2005).

Based on these other viral silencing suppressor, it is worth considering that TGBp1 might also interact with nuclear factors to promote virus infection.

TGBp3:GFP was in the nucleus during PVX infection but is not seen there when expressed alone from pRTL2 plasmids. There may be some amounts of TGBp3 in the nucleus when co-expressed with TGBp1 (Figs. 8H and I). If TGBp1 were responsible for TGBp3 entry to the nucleus, then it would have a dominant effect on TGBp3, blocking ER binding and would chaperone TGBp3 into the nucleus. This would require more than a transient interaction between these two proteins in the cytoplasm, in which case yeast two hybrid experiments should produce positive results. Since the yeast two hybrid experiments were negative, it is reasonable to consider TGBp3 is getting to the nucleus by another mechanism, such as the ER associated degradation (ERAD) pathway. In a recent study of GFP:TGBp2, we found that the fusion protein was degraded more rapidly in PVX-infected protoplasts than when the fusion was expressed in the absence of infection (Ju et al., 2005). We proposed that GFP:TGBp2 was being degraded by the ERAD pathway which involved translocation of the proteins from the ER into the cytosol for proteasome degradation (Ju et al., 2005). This hypothesis was based on a report by Reichel and Beachy (2000) showing that the TMV MP is degraded by the 26S proteasome indicating that ERAD is a factor in virus cell-to-cell movement. Recent studies showed that nuclear accumulation of certain GFP fusions may be a component of ERAD. Proteins that are translocated out of the ER may be actively carried by microtubules into the nucleoplasm (Brandizzi et al., 2003). If the PVX triple gene block proteins are ERAD substrates, then nuclear import may be a feature in controlling protein degradation.

Materials and methods

Bacterial strains and plasmids

All plasmids were constructed using standard cloning techniques (Sambrook et al., 1989) and transformed using *Escherichia coli* strains JM109 or DH5 α . The pPVX-GFP, pPVX-GFP:TGBp1, and pPVX-GFP:TGBp2 plasmids contain the PVX genome next to a bacteriophage T7 promoter as described previously (Fig. 1) (Ju et al., 2005, 2007; Krishnamurthy et al., 2003; Yang et al., 2000). To prepare pPVX-GFP:TGBp1, substitution mutations creating two stop codons at the 5' end of the endogenous PVX TGBp1 coding sequence were introduced into pC2S using the QuikChange[®] II XL Site-Directed Mutagenesis Kit (Stratagene, La Jolla, CA). Forward (GAT TAA GGA CCT TAG GTA GTA CAT GCA GTA GC) and reverse (GCTAC TGC ATG TAC TAC CTA AGG TCC TTA ATC) primers inserted the six nucleotides that are underlined. The mutated pC2S was then digested with *Clai* and *SaII*. GFP:TGBp1 fusion was digested from TXS Δ 25-GFP:TGBp1 with the same enzymes. GFP:TGBp1 was ligated with the mutated pC2S to generate pPVX-GFP:TGBp1. To prepare pPVX-TGBp3:GFP infectious clone, the non-coding region between the TGBp3 and EGFP in pPVX-GFP (Fig. 1) was removed fusing the TGBp3 and EGFP coding sequences.

The triple gene block was PCR amplified using pPVX-GFP, a forward primer (CTT AGA GAT TTG AAT AAG ATG GAT ATT CTC ATC AC) overlapping the TGBp1 translational start codon (underlined), and a reverse primer (CAT GAT CGA TGC TAG ATG GAA ACT TAA CCG TTC) which overlaps the 3' end of TGBp3 and contains a *Clal* site (underlined). The PCR product and the linear pGEM-T Easy vector were ligated (Promega, Madison, WI), creating pGEM-TGB. The pGEM-TGB and pPVX-GFP plasmids were digested with *ApaI* and *Clal* enzymes. The TGB coding sequence and linearized vector were gel purified and ligated creating pPVX.TGBp3-GFP.

Nuclear targeting of the PVX TGBp1 protein was studied using the pRTL2-GUS:TGBp1 and -GUS constructs. To construct the pRTL2-GUS:TGBp1 plasmid, the GFP coding sequence in pRTL2-GFP:TGBp1 was replaced with the β -glucuronidase (GUS) coding sequence. The GUS coding sequence was PCR amplified using the pCXS-GUS plasmid (Chapman et al., 1992). A forward primer (GGCGCC ATG GCA ATG TTA CGT CCT GT) overlapping the 5' end of the GUS gene, which contains added sequences encoding a *NcoI* restriction site (underlined), and a reverse primer (GCG CCG CCC GGG TCA TTG TTT GCC TC) overlapping the 3' end of the GUS gene which contains added sequences encoding a *SmaI* restriction site (underlined) were also used. The PCR products and pRTL2-GFP:TGBp1 plasmids were digested with *NcoI* and *SmaI*, gel purified, and ligated. To prepare pRTL2-GUS, the same 5' primer was used and a reverse primer (TGATGGATCC TCA TTG TTT GCC TCC CTG C) overlapping the 3' end of the GUS gene with a *BamHI* restriction site (underlined) was used. The PCR fragment of GUS gene and the pRTL2 plasmid were digested with *NcoI* and *BamHI*, gel purified, and ligated to generate pRTL2-GUS.

Plasmids containing CFP or Citrine (referred to here as YFP) fused to TGBp1 and TGBp2 were prepared. The pSAT6-ECFP-C1 and pSAT6-Citrine-C1 vectors (provided by Dr. Tzvi Tzfira, State University of New York, Stony Brook, NY) contain tandem CaMV 35S promoters followed by a TEV leader, a multiple cloning site (MCS), and a CaMV 35S transcriptional terminator (Tzfira et al., 2005). To make TGBp1 containing plasmids, TGBp1 was PCR amplified using a forward primer (GCG GTC GAC ATG GAT ATT CTC ATC AGT AGT) containing a *SalI* restriction site (underlined) and a reverse primer (GCG GGA TCC CTA TGG CCC TGC GCG GAC ATA) containing a *BamHI* restriction site (underlined). To make TGBp2 containing plasmids, TGBp2 was PCR amplified using a forward primer (GCG GTC GAC ATG TCC GCG CAG GGC CAT AGG) containing a *SalI* restriction site (underlined) and a reverse primer (GCG GGA TCC CTA ATG ACT GCT ATG ATT GTT) containing a *BamHI* restriction site (underlined). PCR products, pSAT6-CFP-C1, and pSAT6-Citrine-C1 plasmids were digested with *SalI* and *BamHI* and then gel purified. The PCR products and each linearized plasmid were ligated to produce pSAT6-CFP:TGBp1, -CFP:TGBp2, and pSAT6-YFP:TGBp2.

PVX protein–protein interactions were also studied using the Matchmaker Yeast Two-Hybrid System 3 (Clontech, Mountain View, CA). The TGBp1, TGBp2, and TGBp3 coding sequences were PCR amplified from pPVX-GFP and introduced into the

pGBKT7 producing pBD-TGBp1, pBD-TGBp2, and pBD-TGBp3 plasmids. Primers containing additional sequences encoding *NcoI* and *BamHI* restriction sites were used for PCR amplification. The PCR products, pGADT7, and pGBKT7 plasmids were digested with *NcoI* and *BamHI* and then gel purified. The PCR products and linearized pGADT7 vectors were ligated to produce pAD-TGBp1, -TGBp2, and -TGBp3 plasmids. The PCR products and linearized pGBKT7 vectors were ligated to produce pBD-TGBp1, -TGBp2, and -TGBp3 plasmids. The BD designation refers to the bait proteins and the AD designation refers to the prey proteins.

In vitro transcription and plant inoculation

The mMMESSAGE mMACHINE T7 high yield capped RNA transcription kit (Ambion, Inc., Austin, TX) was used to prepare infectious transcripts from the pPVX-GFP, pPVX-GFP:TGBp1, pPVX-GFP:TGBp2, and pPVX-TGBp3:GFP plasmids. *In vitro* transcription reactions were conducted using 1 μ g linearized DNA according to the kit manual. Ten micrograms of each PVX-GFP, PVX.GFP:TGBp1, PVX-GFP:TGBp2, or PVX-TGBp3:GFP transcripts was inoculated to *N. benthamiana* plant dusted with carborundum (Ju et al., 2005, 2007). GFP fluorescence was detected in systemic tissue using a handheld Blak-Ray UV lamp (UV Products, Upland, CA) (Ju et al., 2005).

Preparation and transfection of BY-2 protoplasts

Protoplasts were prepared from actively growing 3- to 5-day-old BY-2 suspension cells as described previously (Ju et al., 2005, 2007). Protoplasts were transfected with either 2 μ l (roughly 30 μ g) infectious transcripts or 5 μ g pRTL2 plasmids plus 40 μ g sonicated salmon sperm DNA (Ju et al., 2005). The transcripts or plasmids were combined with 5×10^5 protoplasts (in 0.5 ml of solution 2) and transferred to a 0.4-cm gap cuvette (Bio-Rad Laboratories, Hercules, CA) on ice. Electroporation was conducted using a Gene Pulser (Bio-Rad Laboratories) at 0.25 kV, 100 Ω , and 125 μ F.

After electroporation, transfected protoplasts were cultured at 26 °C as described previously (Ju et al., 2005, 2007), collected at various time intervals between 12 and 48 h by centrifugation at 59 \times g for 5 min, and then examined using laser scanning confocal microscopy (Ju et al., 2005).

β -Glucuronidase (GUS) assays

One milliliter of media from each well of a 6-well plate containing transfected protoplasts was discarded. Seventy-five microliters of 1 M NaH₂PO₄ pH 7.0, 30 μ l of 50 mM KFeCN, and 20 μ l of 96 mM X-Gluc were added to each well. The cell culture plate was incubated at room temperature under foil for several h to overnight (Restrepo et al., 1990).

Microscopy

A Leica TCS SP2 (Leica Microsystems, Bannockburn, IL) confocal laser scanning microscope system was used to examine

the fluorescence of GFP, CFP, YFP, and RFP. For co-localization studies, we used the Dye Finder software (Leica Microsystems) which detects and removes low-level emissions that may represent a minor portion of the spectrums that can be overlapping. This software was also used to assess whether fluorescent signals overlap or are neighboring. We also used Leica 3-D maximum projection and rotation software to assess whether fluorescent signals were overlapping or adjacent to each other.

GUS activity and ER-tracker dye (Molecular Probes Inc., Eugene, OR) were studied using a Nikon E600 epifluorescence microscope (Nikon Inc., Dallas, TX) equipped with a Magnafire digital camera. GUS is visualized using bright field microscopy. ER-tracker was studied using a UV filter while GFP fluorescence was seen using a blue filter (B2A). ER-tracker has an excitation of 374 nm and emissions spectrum of 430–640 nm, which is not compatible with the UV laser (excitation of 351 nm) on the confocal microscope. All images were processed using Adobe Photoshop version 6.0 software (Adobe Systems Inc., San Jose, CA).

Yeast two-hybrid system

The Matchmaker Yeast Two Hybrid System 3 (Clontech, Mountain View, CA) includes the AH109 yeast strain which has four reporters: *lacZ*, *His3*, *Ade2*, and *Mel1*. Positive and negative control plasmids, pGBKT7-53, pGADT7-T, pCL1, and pGBKT7-Lam, provided by the kit were used. Yeast was transformed with pAD and pBD plasmids and grown according to instructions provided by the kit. Transformants were grown on low stringency medium (SD/–Leu/–Trp). Selected candidates were transferred to medium stringency medium (SD/–Leu/–Trp/–His) or medium stringency medium containing X- α -Gal. Candidates producing a blue reaction in the presence of X- α -Gal were tested in high stringency medium (SD/–Leu/–Trp/–His/–Ade) and in high stringency medium containing X- α -Gal.

Acknowledgments

Support for this project was provided by the National Science Foundation Integrative Plant Biology Program Award IBM-9982252 and in part by the Oklahoma Agriculture Experiment Station under the project H-2371. We thank Drs. R. Matts and S. Hartson for providing the plasmids, protocols, and assistance with in vitro translation and immunoprecipitation experiments. We also thank Terry Colberg for training and assistance with confocal microscope located at the Oklahoma State University Electron Microscopy Center.

References

- Allison, A., Shalla, T., 1973. The ultrastructure of local lesions induced by *Potato virus X*: a sequence of cytological events in the course of infection. *Phytopathology* 64, 784–793.
- Angell, S.M., Davies, C., Baulcombe, D.C., 1996. Cell-to-cell movement of *Potato virus X* is associated with a change in the size-exclusion limit of plasmodesmata in trichome cells of *Nicotiana clevelandii*. *Virology* 216 (1), 197–201.
- Atabekov, J.G., Rodionova, N.P., Karpova, O.V., Kozlovsky, S.V., Poljakov, V.Y., 2000. The movement protein-triggered in situ conversion of *Potato virus X* virion RNA from a nontranslatable into a translatable form. *Virology* 271 (2), 259–263.
- Baulcombe, D., 2002. Viral suppression of systemic silencing. *Trends Microbiol.* 10 (7), 306–308.
- Bayne, E.H., Rakitina, D.V., Morozov, S.Y., Baulcombe, D.C., 2005. Cell-to-cell movement of potato potyvirus X is dependent on suppression of RNA silencing. *Plant J.* 44 (3), 471–482.
- Brandizzi, F., Hanton, S., DaSilva, L.L., Boevink, P., Evans, D., Oparka, K., Denecke, J., Hawes, C., 2003. ER quality control can lead to retrograde transport from the ER lumen to the cytosol and the nucleoplasm in plants. *Plant J.* 34 (3), 269–281.
- Buck, K.W., 1999. Replication of tobacco mosaic virus RNA. *Philos. Trans. R. Soc. Lond., B Biol. Sci.* 354 (1383), 613–627.
- Butterfield-Gerson, K.L., Scheifele, L.Z., Ryan, E.P., Hopper, A.K., Parent, L.J., 2006. Importin-beta family members mediate alpharetrovirus gag nuclear entry via interactions with matrix and nucleocapsid. *J. Virol.* 80 (4), 1798–1806.
- Canto, T., Uhrig, J.F., Swanson, M., Wright, K.M., MacFarlane, S.A., 2006. Translocation of tomato bushy stunt virus P19 protein into the nucleus by ALY proteins compromises its silencing suppressor activity. *J. Virol.* 80 (18), 9064–9072.
- Chapman, S., Kavanagh, T., Baulcombe, D., 1992. *Potato virus X* as a vector for gene expression in plants. *Plant J.* 2 (4), 549–557.
- Cowan, G.H., Lioliopoulou, F., Ziegler, A., Torrance, L., 2002. Subcellular localisation, protein interactions, and RNA binding of potato mop-top virus triple gene block proteins. *Virology* 298 (1), 106–115.
- Crawford, K.M., Zambryski, P.C., 1999. Plasmodesmata signaling: many roles, sophisticated statuses. *Curr. Opin. Plant Biol.* 2 (5), 382–387.
- Crawford, K.M., Zambryski, P.C., 2001. Non-targeted and targeted protein movement through plasmodesmata in leaves in different developmental and physiological states. *Plant Physiol.* 125 (4), 1802–1812.
- Davies, C., Hills, G., Baulcombe, D.C., 1993. Sub-cellular localization of the 25-kDa protein encoded in the triple gene block of *Potato virus X*. *Virology* 197 (1), 166–175.
- DeVries, T.A., Neville, M.C., Reyland, M.E., 2002. Nuclear import of PKCdelta is required for apoptosis: identification of a novel nuclear import sequence. *EMBO J.* 21 (22), 6050–6060.
- Dixit, R., Cyr, R., 2002. Golgi secretion is not required for marking the preprophase band site in cultured tobacco cells. *Plant J.* 29 (1), 99–108.
- Erhardt, M., Stussi-Garaud, C., Guilley, H., Richards, K.E., Jonard, G., Bouzoubaa, S., 1999. The first triple gene block protein of peanut clump virus localizes to the plasmodesmata during virus infection. *Virology* 264 (1), 220–229.
- Erhardt, M., Morant, M., Ritzenthaler, C., Stussi-Garaud, C., Guilley, H., Richards, K., Jonard, G., Bouzoubaa, S., Gilmer, D., 2000. P42 movement protein of beet necrotic yellow vein virus is targeted by the movement proteins P13 and P15 to punctate bodies associated with plasmodesmata. *Mol. Plant-Microb. Interac.* 13 (5), 520–528.
- Erhardt, M., Vetter, G., Gilmer, D., Bouzoubaa, S., Richards, K., Jonard, G., Guilley, H., 2005. Subcellular localization of the triple gene block movement proteins of Beet necrotic yellow vein virus by electron microscopy. *Virology* 340 (1), 155–166.
- Espinoza, A.M., Medina, V., Hull, R., Markham, P.G., 1991. Cauliflower mosaic virus gene II product forms distinct inclusion bodies in infected plant cells. *Virology* 185 (1), 337–344.
- Gilmer, D., Bouzoubaa, S., Hehn, A., Guilley, H., Richards, K., Jonard, G., 1992. Efficient cell-to-cell movement of beet necrotic yellow vein virus requires 3' proximal genes located on RNA 2. *Virology* 189 (1), 40–47.
- Gorshkova, E.N., Erokhina, T.N., Stroganova, T.A., Yelina, N.E., Zamyatin Jr., A.A., Kalinina, N.O., Schiemann, J., Solovyev, A.G., Morozov, S.Y., 2003. Immunodetection and fluorescent microscopy of transgenically expressed hordeivirus TGBp3 movement protein reveals its association with endoplasmic reticulum elements in close proximity to plasmodesmata. *J. Gen. Virol.* 84 (Pt. 4), 985–994.
- Haupt, S., Cowan, G.H., Ziegler, A., Roberts, A.G., Oparka, K.J., Torrance, L., 2005. Two plant-viral movement proteins traffic in the endocytic recycling pathway. *Plant Cell* 17 (1), 164–181.

- Howard, A.R., Heppler, M.L., Ju, H.-J., Krishnamurthy, K., Payton, M.E., Verchot-Lubicz, J., 2004. *Potato virus X* TGBp1 induces plasmodesmata gating and moves between cells in several host species whereas CP moves only in *N. benthamiana* leaves. *Virology* 328, 185–197.
- Hsu, H.T., Hsu, Y.H., Bi, I.P., Lin, N.S., Chang, B.Y., 2004. Biological functions of the cytoplasmic TGBp1 inclusions of bamboo mosaic potexvirus. *Arch. Virol.* 149 (5), 1027–1035.
- Ju, H.J., Samuels, T.D., Wang, Y.S., Blancaflor, E., Payton, M., Mitra, R., Krishnamurthy, K., Nelson, R.S., Verchot-Lubicz, J., 2005. The *Potato virus X* TGBp2 movement protein associates with endoplasmic reticulum-derived vesicles during virus infection. *Plant Physiol.* 138 (4), 1877–1895.
- Ju, H.J., Brown, J.E., Ye, C.M., Verchot-Lubicz, J., 2007. Mutations in the central domain of *Potato virus X* TGBp2 eliminate granular vesicles and virus cell-to-cell trafficking. *J. Virol.* 81 (4), 1899–1911.
- Kalinina, N.O., Fedorkin, O.N., Samuilova, O.V., Maiss, E., Korpela, T., Morozov, S., Atabekov, J.G., 1996. Expression and biochemical analyses of the recombinant *Potato virus X* 25K movement protein. *FEBS Lett.* 397 (1), 75–78.
- Kalinina, N.O., Rakitina, D.V., Solovyev, A.G., Schiemann, J., Morozov, S.Y., 2002. RNA helicase activity of the plant virus movement proteins encoded by the first gene of the triple gene block. *Virology* 296 (2), 321–329.
- Kikumoto, T., Matsui, C., 1961. Electron microscopy of intracellular *Potato virus X*. *Virology* 13, 294–299.
- Kiselyova, O.I., Yaminsky, I.V., Karger, E.M., Frolova, O.Y., Dorokhov, Y.L., Atabekov, J.G., 2001. Visualization by atomic force microscopy of tobacco mosaic virus movement protein–RNA complexes formed in vitro. *J. Gen. Virol.* 82 (Pt. 6), 1503–1508.
- Kiselyova, O.I., Yaminsky, I.V., Karpova, O.V., Rodionova, N.P., Kozlovsky, S.V., Arkhipenko, M.V., Atabekov, J.G., 2003. AFM study of *Potato virus X* disassembly induced by movement protein. *J. Mol. Biol.* 332 (2), 321–325.
- Kozar, F.E., Sheludko, Y.M., 1969. Ultrastructure of potato and *Datura stramonium* plant cells infected with *Potato virus X*. *Virology* 38, 220–229.
- Krishnamurthy, K., Mitra, R., Payton, M.E., Verchot-Lubicz, J., 2002. Cell-to-cell movement of the PVX 12K, 8K, or coat proteins may depend on the host, leaf developmental stage, and the PVX 25K protein. *Virology* 300 (2), 269–281.
- Krishnamurthy, K., Heppler, M., Mitra, R., Blancaflor, E., Payton, M., Nelson, R.S., Verchot-Lubicz, J., 2003. The *Potato virus X* TGBp3 protein associates with the ER network for virus cell-to-cell movement. *Virology* 309 (1), 135–151.
- Lauber, E., Bleykasten-Grosshans, C., Erhardt, M., Bouzoubaa, S., Jonard, G., Richards, K.E., Guilley, H., 1998. Cell-to-cell movement of beet necrotic yellow vein virus: I. Heterologous complementation experiments provide evidence for specific interactions among the triple gene block proteins. *Mol. Plant-Microb. Interact.* 11 (7), 618–625.
- Lawrence, D.M., Jackson, A.O., 2001. Interactions of the TGB1 protein during cell-to-cell movement of barley stripe mosaic virus. *J. Virol.* 75 (18), 8712–8723.
- Lough, T.J., Shash, K., Xoconostle-Cázares, B., Hofstra, K.R., Beck, D.L., Balmori, E., Forster, R.L.S., Lucas, W.J., 1998. Molecular dissection of the mechanism by which potexvirus triple gene block proteins mediate cell-to-cell transport of infectious RNA. *Molec. Plant-Microb. Interact.* 11, 801–814.
- Lough, T.J., Netzler, N.E., Emerson, S.J., Sutherland, P., Carr, F., Beck, D.L., Lucas, W.J., Forster, R.L., 2000. Cell-to-cell movement of potexviruses: evidence for a ribonucleoprotein complex involving the coat protein and first triple gene block protein. *Mol. Plant-Microb. Interact.* 13 (9), 962–974.
- Lucas, W.J., 2006. Plant viral movement proteins: agents for cell-to-cell trafficking of viral genomes. *Virology* 344 (1), 169–184.
- Lucy, A.P., Guo, H.S., Li, W.X., Ding, S.W., 2000. Suppression of post-transcriptional gene silencing by a plant viral protein localized in the nucleus. *EMBO J.* 19 (7), 1672–1680.
- Memelink, J., van der Vlugt, C.I., Linthorst, H.J., Derks, A.F., Asjes, C.J., Bol, J.F., 1990. Homologies between the genomes of a carlavirus (lily symptomless virus) and a potexvirus (lily virus X) from lily plants. *J. Gen. Virol.* 71 (Pt. 4), 917–924.
- Mitra, R., Krishnamurthy, K., Blancaflor, E., Payton, M., Nelson, R.S., Verchot-Lubicz, J., 2003. The *Potato virus X* TGBp2 protein association with the endoplasmic reticulum plays a role in but is not sufficient for viral cell-to-cell movement. *Virology* 312 (1), 35–48.
- Morozov, S.Y., Solovyev, A.G., 2003. Triple gene block: modular design of a multifunctional machine for plant virus movement. *J. Gen. Virol.* 84 (Pt. 6), 1351–1366.
- Morozov, S.Y., Solovyev, A.G., Kalinina, N.O., Fedorkin, O.N., Samuilova, O.V., Schiemann, J., Atabekov, J.G., 1999. Evidence for two nonoverlapping functional domains in the *Potato virus X* 25K movement protein. *Virology* 260 (1), 55–63.
- Oparka, K.J., Roberts, A.G., Roberts, I.M., Prior, D.A.M., Santa Cruz, S., 1996. Viral coat protein is targeted to, but does not gate, plasmodesmata during cell-to-cell movement of *Potato virus X*. *Plant J.* 10, 805–813.
- Oparka, K.J., Prior, D.A., Santa Cruz, S., Padgett, H.S., Beachy, R.N., 1997. Gating of epidermal plasmodesmata is restricted to the leading edge of expanding infection sites of tobacco mosaic virus (TMV). *Plant J.* 12 (4), 781–789.
- Oparka, K.J., Roberts, A.G., Boevink, P., Santa Cruz, S., Roberts, I., Pradel, K.S., Imlau, A., Kotlizky, G., Sauer, N., Epel, B., 1999. Simple, but not branched, plasmodesmata allow the nonspecific trafficking of proteins in developing tobacco leaves. *Cell* 97 (6), 743–754.
- Padgett, H.S., Epel, B.L., Kahn, T.W., Heinlein, M., Watanabe, Y., Beachy, R. N., 1996. Distribution of tobamovirus movement protein in infected cells and implications for cell-to-cell spread of infection. *Plant J.* 10 (6), 1079–1088.
- Reichel, C., Beachy, R.N., 2000. Degradation of Tobacco mosaic virus movement protein by the 26S proteasome. *J. Virol.* 74, 3330–3337.
- Reiser, V., Ruis, H., Ammerer, G., 1999. Kinase activity-dependent nuclear export opposes stress-induced nuclear accumulation and retention of Hog1 mitogen-activated protein kinase in the budding yeast *Saccharomyces cerevisiae*. *Mol. Biol. Cell* 10 (4), 1147–1161.
- Restrepo, M.A., Freed, D.D., Carrington, J.C., 1990. Nuclear transport of plant potyviral proteins. *Plant Cell* 2 (10), 987–998.
- Rodionova, N.P., Karpova, O.V., Kozlovsky, S.V., Zayakina, O.V., Arkhipenko, M.V., Atabekov, J.G., 2003. Linear remodeling of helical virus by movement protein binding. *J. Mol. Biol.* 333 (3), 565–572.
- Rouleau, M., Smith, R.J., Bancroft, J.B., Mackie, G.A., 1994. Purification, properties, and subcellular localization of foxtail mosaic potexvirus 26-kDa protein. *Virology* 204 (1), 254–265.
- Sambrook, J., Fritsch, E.F., Maniatis, T., 1989. *Molecular Cloning: A Laboratory Manual*, 2nd ed. Cold Spring Harbor Press, Cold Spring Harbor, NY.
- SantaCruz, S., Chapman, S., Roberts, A.G., Roberts, I.M., Prior, D.A., Oparka, K.J., 1996. Assembly and movement of a plant virus carrying a green fluorescent protein overcoat. *Proc. Natl. Acad. Sci. U.S.A.* 93 (13), 6286–6290.
- SantaCruz, S., Roberts, A.G., Prior, D.A., Chapman, S., Oparka, K.J., 1998. Cell-to-cell and phloem-mediated transport of *Potato virus X*. The role of virions. *Plant Cell* 10 (4), 495–510.
- Schepetilnikov, M.V., Manske, U., Solovyev, A.G., Zamyatin Jr., A.A., Schiemann, J., Morozov, S.Y., 2005. The hydrophobic segment of *Potato virus X* TGBp3 is a major determinant of the protein intracellular trafficking. *J. Gen. Virol.* 86 (Pt. 8), 2379–2391.
- Skryabin, K.G., Morozov, S., Kraev, A.S., Rozanov, M.N., Chernov, B.K., Lukasheva, L.I., Atabekov, J.G., 1988. Conserved and variable elements in RNA genomes of potexviruses. *FEBS Lett.* 240 (1–2), 33–40.
- Solovyev, A.G., Stroganova, T.A., Zamyatin Jr., A.A., Fedorkin, O.N., Schiemann, J., Morozov, S.Y., 2000. Subcellular sorting of small membrane-associated triple gene block proteins: TGBp3-assisted targeting of TGBp2. *Virology* 269 (1), 113–127.
- Tamai, A., Meshi, T., 2001. Cell-to-cell movement of *Potato virus X*: the role of p12 and p8 encoded by the second and third open reading frames of the triple gene block. *Mol. Plant-Microb. Interact.* 14 (10), 1158–1167.
- Tzfira, T., Tian, G.W., Lacroix, B., Vyas, S., Li, J., Leitner-Dagan, Y., Krichevsky, A., Taylor, T., Vainstein, A., Citovsky, V., 2005. pSAT vectors: a modular series of plasmids for autofluorescent protein tagging and expression of multiple genes in plants. *Plant Mol. Biol.* 57 (4), 503–516.

- Uhrig, J.F., Canto, T., Marshall, D., MacFarlane, S.A., 2004. Relocalization of nuclear ALY proteins to the cytoplasm by the tomato bushy stunt virus P19 pathogenicity protein. *Plant Physiol.* 135 (4), 2411–2423.
- Voinnet, O., Lederer, C., Baulcombe, D.C., 2000. A viral movement protein prevents spread of the gene silencing signal in *Nicotiana benthamiana*. *Cell* 103 (1), 157–167.
- Wang, H., Hao, L., Shung, C.Y., Sunter, G., Bisaro, D.M., 2003. Adenosine kinase is inactivated by geminivirus AL2 and L2 proteins. *Plant Cell* 15 (12), 3020–3032.
- Wang, H., Buckley, K.J., Yang, X., Buchmann, R.C., Bisaro, D.M., 2005. Adenosine kinase inhibition and suppression of RNA silencing by geminivirus AL2 and L2 proteins. *J. Virol.* 79 (12), 7410–7418.
- Yang, Y., Ding, B., Baulcombe, D.C., Verchot, J., 2000. Cell-to-cell movement of the 25K protein of *Potato virus X* is regulated by three other viral proteins. *Mol. Plant-Microb. Interact.* 13 (6), 599–605.
- Yelina, N.E., Erokhina, T.N., Lukhovitskaya, N.I., Minina, E.A., Schepetilnikov, M.V., Lesemann, D.E., Schiemann, J., Solovyev, A.G., Morozov, S.Y., 2005. Localization of poa semilatifolius virus cysteine-rich protein in peroxisomes is dispensable for its ability to suppress RNA silencing. *J. Gen. Virol.* 86 (Pt. 2), 479–489.
- Zambryski, P., 2004. Cell-to-cell transport of proteins and fluorescent tracers via plasmodesmata during plant development. *J. Cell Biol.* 164 (2), 165–168.
- Zamyatnin Jr., A.A., Solovyev, A.G., Sablina, A.A., Agranovsky, A.A., Katul, L., Vetten, H.J., Schiemann, J., Hinkkanen, A.E., Lehto, K., Morozov, S.Y., 2002. Dual-colour imaging of membrane protein targeting directed by poa semilatifolius virus movement protein TGBp3 in plant and mammalian cells. *J. Gen. Virol.* 83 (Pt. 3), 651–662.
- Zamyatnin Jr., A.A., Solovyev, A.G., Savenkov, E.I., Germundsson, A., Sandgren, M., Valkonen, J.P., Morozov, S.Y., 2004. Transient coexpression of individual genes encoded by the triple gene block of potato mop-top virus reveals requirements for TGBp1 trafficking. *Mol. Plant-Microb. Interact.* 17 (8), 921–930.
- Zamyatnin Jr., A.A., Solovyev, A.G., Bozhkov, P.V., Valkonen, J.P., Morozov, S.Y., Savenkov, E.I., 2006. Assessment of the integral membrane protein topology in living cells. *Plant J.* 46 (1), 145–154.